Neurobiology:

The Neuroendocrine Protein 7B2 Suppresses the Aggregation of Neurodegenerative Disease-related Proteins

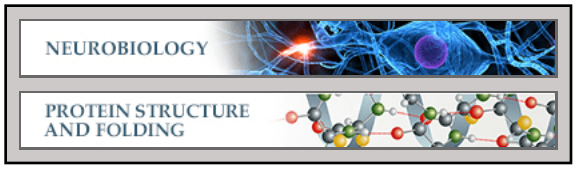

Michael Helwig, Akina Hoshino, Casey Berridge, Sang-Nam Lee, Nikolai Lorenzen, Daniel E. Otzen, Jason L. Eriksen and Iris Lindberg

J. Biol. Chem. 2013, 288:1114-1124.
doi: 10.1074/jbc.M112.417071 originally published online November 21, 2012

Access the most updated version of this article at doi: 10.1074/jbc.M112.417071

Find articles, minireviews, Reflections and Classics on similar topics on the JBC Affinity Sites.

Alerts:
- When this article is cited
- When a correction for this article is posted

Click here to choose from all of JBC's e-mail alerts

This article cites 53 references, 18 of which can be accessed free at
http://www.jbc.org/content/288/2/1114.full.html#ref-list-1

Downloaded from http://www.jbc.org/ at YONSEI UNIVERSITY on May 20, 2014

THE JOURNAL OF BIOLOGICAL CHEMISTRY VOL. 288, NO. 2, pp. 1114–1124, January 11, 2013
© 2013 by The American Society for Biochemistry and Molecular Biology, Inc. Published in the U.S.A.

The Neuroendocrine Protein 7B2 Suppresses the Aggregation of Neurodegenerative Disease-related Proteins*

Received for publication, September 7, 2012, and in revised form, November 11, 2012 Published, JBC Papers in Press, November 21, 2012, DOI 10.1074/jbc.M112.417071

Michael Helwig[‡], Akina Hoshino[‡], Casey Berridge[§], Sang-Nam Lee[¶], Nikolai Lorenzen[‖], Daniel E. Otzen[‖], Jason L. Eriksen[§], and Iris Lindberg[‡1]

From the [‡]Department of Anatomy and Neurobiology, University of Maryland School of Medicine, Baltimore, Maryland 21201, the [§]Department of Pharmacological and Pharmaceutical Sciences, College of Pharmacy, University of Houston, Houston, Texas 77204, the [¶]Research Center for Natural Human Defense System, Yonsei University College of Medicine, Seoul 120-752, Korea, and the [‖]Department of Molecular Biology and Genetics, Interdisciplinary Nanoscience Centre, Aarhus University, 8000 Aarhus C, Denmark

Background: The neuroendocrine protein 7B2 blocks the aggregation of certain secreted proteins.
Results: 7B2 co-localizes with protein aggregates in Parkinson and Alzheimer disease brains; blocks the fibrillation of $A\beta_{1-40}$, $A\beta_{1-42}$, and α-synuclein; and blocks $A\beta_{1-42}$-induced Neuro-2A cell death.
Conclusion: 7B2 inhibits the cytotoxicity of $A\beta_{1-42}$ by modulation of oligomer formation.
Significance: 7B2 is a novel anti-aggregation secretory chaperone associated with neurodegenerative disease.

Neurodegenerative diseases such as Alzheimer (AD) and Parkinson (PD) are characterized by abnormal aggregation of misfolded β-sheet-rich proteins, including amyloid-β (Aβ)-derived peptides and tau in AD and α-synuclein in PD. Correct folding and assembly of these proteins are controlled by ubiquitously expressed molecular chaperones; however, our understanding of neuron-specific chaperones and their involvement in the pathogenesis of neurodegenerative diseases is limited. We here describe novel chaperone-like functions for the secretory protein 7B2, which is widely expressed in neuronal and endocrine tissues. In *in vitro* experiments, 7B2 efficiently prevented fibrillation and formation of $A\beta_{1-42}$, $A\beta_{1-40}$, and α-synuclein aggregates at a molar ratio of 1:10. In cell culture experiments, inclusion of recombinant 7B2, either in the medium of Neuro-2A cells or intracellularly via adenoviral 7B2 overexpression, blocked the neurocytotoxic effect of $A\beta_{1-42}$ and significantly increased cell viability. Conversely, knockdown of 7B2 by RNAi increased $A\beta_{1-42}$-induced cytotoxicity. In the brains of APP/PSEN1 mice, a model of AD amyloidosis, immunoreactive 7B2 co-localized with aggregation-prone proteins and their respective aggregates. Furthermore, in the hippocampus and substantia nigra of human AD- and PD-affected brains, 7B2 was highly co-localized with Aβ plaques and α-synuclein deposits, strongly suggesting physiological association. Our data provide insight into novel functions of 7B2 and establish this neural protein as an anti-aggregation chaperone associated with neurodegenerative disease.

Excessive aggregation of misfolded proteins is a common feature in the pathophysiology of many neurodegenerative disorders such as Alzheimer disease (AD),[2] Parkinson disease (PD), and amyotrophic lateral sclerosis (1). AD, for example, is neuroanatomically characterized by extracellular plaques composed of amyloid precursor protein (APP)-derived amyloid-β (Aβ) peptides (2) and intracellular neurofibrillary tangles made up of hyperphosphorylated tau (3). Similarly, Lewy bodies, the hallmark of PD, are large cytosolic inclusion bodies composed of aggregated α-synuclein protein within dopaminergic neurons of the substantia nigra (4). Although the exact pathogenic role of these various aggregates is incompletely understood, it has been hypothesized that aggregation of Aβ peptides into oligomers and plaques results in a neurotoxic environment, disrupting cell function and leading to the loss of specific neuronal populations (5).

In the search for the underlying molecular mechanisms for these toxic effects, chaperone proteins have been implicated as important modulators of abnormal protein folding and aggregation in various neurodegenerative diseases (6). For example, several ubiquitously expressed molecular chaperones within the heat shock (*e.g.* HSP90, HSP70, and HSP27) and α-crystallin protein families have been shown to be associated with protein-misfolding diseases (7–10). The secreted chaperone clusterin has also been implicated in neurodegenerative disease (reviewed in Refs. 11 and 12). However, our understanding of the role of chaperone-mediated quality control machinery in neurodegenerative disease is still limited, and the question of whether chaperones other than heat shock proteins, crystallins, and clusterin might contribute to plaque pathogenesis or clearance remains open.

The secretory protein 7B2, known best for its role as a prohormone convertase 2 (proPC2)-binding protein (13, 14), is universally expressed in endocrine, neural, and neuroendocrine

* This work was supported, in whole or in part, by National Institutes of Health Grants 1R01DK49703 (to I. L.) and 1R15AG039008 (to J. L. E.). This work was also supported by Alzheimer's Association Grant NIRG-08-92033 (to J. L. E.), the Michael J. Fox Foundation for Parkinson's Research (to N. L. and D. E. O.), and German Academy of Sciences Leopoldina Foundation Postdoctoral Grant LPDS 2009-33 (to M. H.).
⌘ *Author's Choice*—Final version full access.
[1] To whom correspondence should be addressed: Dept. of Anatomy and Neurobiology, University of Maryland School of Medicine, HSF II, Rm. S251, 20 Penn St., Baltimore, MD 21201. Tel.: 410-706-4778; Fax: 410-706-2512; E-mail: ilind001@umaryland.edu.

[2] The abbreviations used are: AD, Alzheimer disease; PD, Parkinson disease; APP, amyloid precursor protein; Aβ, amyloid-β; ThT, thioflavin T.

Downloaded from http://www.jbc.org/ at YONSEI UNIVERSITY on May 20, 2014

cells, which all possess a regulated secretory pathway (15, 16). Because expression of 7B2 in the brain is not confined to convertase-containing neurons (15), it seems likely that 7B2 must possess physiological functions exceeding its involvement in neuropeptide synthesis. Early reports indicated that 7B2 could be distantly related to a subclass of molecular chaperones called chaperonins (17). 7B2 blocks the formation of proPC2 oligomers and aggregates (18) as well as IGF-1 aggregates (19), demonstrating that 7B2 functions as a post-folding and post-secretion chaperone. Moreover, independent discovery studies searching for biomarkers of early-onset AD, PD, and amyotrophic lateral sclerosis have identified 7B2 as a potential candidate protein (20–23).

On the basis of findings showing association of 7B2 with neurodegenerative disease and the known role of 7B2 in blocking proPC2 aggregation, we investigated the hypothesis that neuronal 7B2 could function to block neurodegenerative disease-related protein aggregation. We tested the action of 7B2-derived proteins on the cytotoxicity and fibrillation of the $A\beta_{1-42}$ and $A\beta_{1-40}$ peptides and α-synuclein. Our experiments using animal, cellular, and *in vitro* approaches provide collective support for the idea that 7B2 represents a novel neuroprotective chaperone.

EXPERIMENTAL PROCEDURES

Animal Models—All studies were conducted following University of Houston-approved Institutional Animal Care and Use Committee protocols. B6C6-Tg(APPswe,PSEN1dE9)85Dbo/J (APP/PSEN1; The Jackson Laboratory) mice (12 months old) were used in this study. APP/PSEN1 double transgenic mice express a chimeric mouse/human APP (Mo/HuAPP695swe) and a mutant human presenilin-1 (PS1-dE9) protein, both directed to CNS neurons; these familial mutations are strongly associated with early-onset AD. The mice were killed, and the brains were fixed with Accustain (Sigma) and subjected to paraffin processing. Brains were sectioned using a Leica microtome at 10-μm intervals.

Immunohistochemistry of Mouse Brain Tissue—Coronal sections (10 μm) of formalin-fixed tissue were deparaffinized and subjected to an antigen retrieval protocol using Aqua DePar and Reveal antigen retrieval solutions in a Decloaking Chamber system (Biocare Medical). Following antigen retrieval, some sections were briefly stained with methoxy-X04 (1 μM), followed by extensive washing to visualize dense core amyloid pathology. Other sections were treated with an avidin/biotin blocking kit (Vector Laboratories, Burlingame, CA), followed by treatment with 5% normal goat serum in Tris-buffered saline containing 0.5% Tween 20 (TBST) for 20 min. Sections were incubated with polyclonal rabbit anti-7B2 antiserum (LSU13BF; 1:200) for 1 h and washed with TBST. Sections were incubated with biotinylated goat anti-rabbit antibody (Vector Laboratories) for 30 min, washed with TBST, and then incubated with Texas Red-labeled avidin DCS (Vector Laboratories) for 10 min. Sections were then washed with TBST. For co-localization, tissue was reblocked using the avidin/biotin blocking kit, subjected to a second round of blocking, and incubated with a second round of antibodies (anti-$A\beta_{1-42}$; 12F4; 1:250; Covance), followed by washing and incubation with fluorescein-avidin (Vector Laboratories) for 10 min. The sections were then washed extensively with Tris-HCl, mounted using VECTASHIELD medium, and viewed under an Olympus IX61 DSU confocal microscope. Images were processed with Neurolucida (MicroBrightField, Inc., Williston, VT).

Human Brain Tissues—An AD-affected human brain sample (73-year-old female donor) and a control sample (72-year-old male donor, naturally deceased) containing the hippocampus and a PD-affected human midbrain sample containing the substantia nigra of a 89-year-old male donor were obtained from the NICHD Brain and Tissue Bank for Developmental Disorders of the University of Maryland, Baltimore. Formalin-fixed brain samples at either the level of the cortex or mesencephalon, respectively, were cryoprotected in 30% sucrose, deep-frozen in isopentane over dry ice (1 min), and stored at −80 °C until required.

Immunohistochemistry of Human Brain Tissue—Coronal sections (16 μm) containing the hippocampus (AD and control samples) and the substantia nigra (PD sample) were processed using a Leica cryostat, collected on Superfrost Plus object slides (Fisher Scientific, Hampton, NH), and treated with blocking solution containing 3% BSA in 0.5% Triton X-100 in PBS (0.5% PBST) for 1 h to block nonspecific reactions. Sections were then incubated with polyclonal rabbit anti-7B2 antiserum (LSU13BF; 1:250) and monoclonal mouse anti-α-synuclein antiserum (1:150; BD Biosciences) (24) in blocking solution overnight at 4 °C. Sections were rinsed briefly with 0.25% PBST and PBS and incubated with Cy3-conjugated (Ex_{max} = 550 nm and Em_{max} = 570 nm) goat anti-rabbit (A10520; 1:200; Invitrogen) and Cy2-conjugated (Ex_{max} = 492 nm and Em_{max} = 510 nm) donkey anti-mouse (AP124J; 1:250; Millipore) secondary antibodies in blocking solution containing H33342 (Ex_{max} = 350 nm and Em_{max} = 461 nm) nuclear/DNA staining reagent (1:10,000; ALX-620-050, Axxora LLC, San Diego, CA) for 2 h at room temperature. Sections were rinsed with PBS and coverslipped with Fluoromount G (Electron Microscopy Sciences, Hatfield, PA). Immunofluorescence was visualized using an Olympus BX61 confocal microscope and a Nikon Eclipse TE2000-E epifluorescence microscope. Images of immunoreactivity were merged by color channel overlay using microscope-specific image processing software (Olympus FluoView and Nikon MetaView). Anatomical localization of immunoreactivity within the brain was annotated according to the Allen Human Brain Atlas Data Portal and *Gray's Anatomy of the Human Body* (54).

$A\beta_{1-42}$ Oligomer Preparation—$A\beta_{1-42}$ peptide films were resuspended in Me_2SO at a concentration of 5 mM, and the peptide solutions were sonicated in a water bath sonicator for 10 min at room temperature. The solutions were then diluted to a final concentration of 100 μM with Ham's F-12 medium (phenol red-free; BIOSOURCE) and incubated at 4 °C for 24 h to form $A\beta_{1-42}$ oligomers (25). In some experiments, $A\beta_{1-42}$ oligomers were added to the medium of Neuro-2A cells in the presence of vehicle (Ham's F-12), recombinant 7B2 (see below), α-crystallin (Sigma), or α-lactalbumin (14.2 kDa; L4385, Sigma).

Cell Proliferation and Viability Assay—Neuro-2A cells were seeded at 5×10^3/well in 96-well plates and left to attach at

Downloaded from http://www.jbc.org/ at YONSEI UNIVERSITY on May 20, 2014

37 °C overnight. Subsequently, cells were treated with 10 μM $A\beta_{1-42}$ oligomers in the presence or absence of 2–4 μM 7B2, α-lactalbumin as a negative control, or vehicle (Ham's F-12) for 48 h. Cell survival was measured at the indicated times by adding 10 μl of a 1:3 (v/v) diluted WST-1 cell proliferation reagent stock solution (Roche Applied Science). Samples were incubated for 60–240 min, and absorbance at 450 nm was measured with a SpectraMax M2 fluorometer (Molecular Devices, Sunnyvale, CA) using a 690-nm reference filter. After subtraction of the background absorbance, the mean values of the untreated control cells were set as 100%. In addition, cell viability was assessed by labeling cells with calcein AM (2 μM; Ex_{max} = 485 nm and Em_{max} = 530 nm; L3224, Invitrogen), and fluorescence was measured using the SpectraMax M2 fluorometer. Representative photomicrographs were taken using the Nikon Eclipse TE2000-E epifluorescence microscope.

Adenoviral Infection of Neuro-2A Cells—To infect Neuro-2A cells with 7B2-encoding adenovirus (26), cells were seeded at 5×10^3/well into 96-well plates. Replicate wells were trypsinized and counted again the following day for calculation of adenoviral multiplicity of infection. Cells were washed twice with PBS, and 7B2 or control (β-galactosidase-encoding) adenovirus was diluted to achieve a multiplicity of infection of 1 in PBS in a final volume of 50 μl/well. The diluted adenovirus solution was added directly to cells in growth medium, and the plates were swirled to mix well and incubated for 30 min to permit adenoviral infection. Fifty μl of high glucose DMEM containing 2% fetal bovine serum were then added to each well. Adenovirus-infected cells were incubated for 36 h at 37 °C in a CO_2 incubator. The medium was then changed to DMEM containing 10 μM $A\beta_{1-42}$ for 48 h. Cell viability was assessed at this time using the WST-1 cell proliferation assay as described above.

7B2 RNAi Experiments—Three different specific sequences of Stealth siRNA (Invitrogen) were designed for the murine 7B2 mRNA sequence (MSS237887, MSS237888, and MSS237889). Following assessment of individual knockdown efficiencies, the most effective siRNA, MSS237887, was deployed. A control scrambled sequence was designed to have the same GC content (46-2000, Invitrogen). Neuro-2A cells grown in 96-well plates were transfected sequentially with the respective siRNA at 100 nM on the first day and 200 nM on the second day using 5 μl/well Lipofectamine 2000 (Invitrogen). The medium was then changed overnight to DMEM containing 4 μM $A\beta_{1-42}$ for 48 h. Transfection efficiency in Neuro-2A cells was monitored using a scrambled siRNA sequence conjugated to fluorescein (N2100S, New England Biolabs). The total cell number was determined by counterstaining with 5 μg/ml Hoechst 33342 (Invitrogen) for 45 min and subsequent examination by fluorescence microscopy. Cell viability was assessed using the WST-1 cell proliferation assay as described above.

Cellular Uptake of 7B2 and $A\beta_{1-42}$ into Neuro-2A Cells—Neuro-2A cells were grown overnight in 24-well plates on coverslips in DMEM supplemented with 10% (v/v) fetal bovine serum. On the next day, 250 nM Alexa Fluor 647-labeled $A\beta_{1-42}$ (64161, AnaSpec, Fremont, CA) and recombinant 7B2 were added to the medium, and cells were incubated at 37 °C in 5% CO_2 for 24 h. Neuro-2A cells were then treated with 4% paraformaldehyde for 20 min and incubated with blocking solution containing 3% BSA in 0.5% PBST for 1 h to block nonspecific reactions. Exogenous 7B2 was then visualized using Alexa Fluor 488-labeled anti-His tag antibody (16-254, Millipore). Cells were rinsed briefly with 0.25% PBST and PBS containing DAPI (Ex_{max} = 358 nm and Em_{max} = 461 nm) nuclear/DNA staining reagent (1:10,000; D1306, Invitrogen) for 2 h at room temperature. Cells were then rinsed with PBS and mounted on object slides with Fluoromount G. Immunofluorescence was visualized using the Olympus BX61 confocal microscope and the Nikon Eclipse TE2000-E epifluorescence microscope.

Peptide Synthesis and Purification of Recombinant 7B2-derived Peptides—An automated bench-top simultaneous multiple solid-phase peptide synthesizer (PSSM-8 system, Shimadzu) was used for the synthesis of 7B2 peptide 86–121 by the *N*-(9-fluorenyl)methoxycarbonyl (Fmoc) procedure in NovaSyn TGR resin (Novabiochem, San Diego, CA) as described previously (27). The molecular mass and purity of the synthetic peptide were verified by reverse-phase HPLC and matrix-assisted laser desorption/ionization time-of-flight mass spectrometry (TofSpec E, Micromass). Recombinant His-tagged 27- and 21-kDa 7B2 and 7B2 peptides 30–150 and 68–150 were prepared using the QIAexpress system (Qiagen). Primers were designed as described previously (27). PCR fragments were cloned into pQE30, and sequences were verified by DNA sequencing. Proteins were expressed in *Escherichia coli* XL1-Blue (Stratagene) and purified with the guanidine HCl/refolding method as described previously (28).

Thioflavin T Assay—Fibrillation of amylogenic peptides ($A\beta_{1-42}$, $A\beta_{1-40}$, and α-synuclein) in the presence and absence of 7B2 was measured by thioflavin T (ThT) fluorescence assays in 96-well plates (29). Recombinant $A\beta_{1-42}$ and $A\beta_{1-40}$ were purchased from Biopeptide Co. (San Diego, CA), and α-synuclein was expressed and purified as described (30). $A\beta_{1-40}$ and $A\beta_{1-42}$ were diluted in 0.5% Me_2SO and 0.5 M Tris-HCl buffer (pH 7.4; 1 mg/ml) and then diluted into 40 μM ThT solutions (in quadruplicate) containing or lacking the various forms of 7B2 in a total volume of 100 μl. α-Synuclein fibrillation assays were performed in PBS (pH 7.4) and included one 3/32-inch diameter polytetrafluoroethylene bead (McMaster-Carr, Santa Fe Springs, CA) per well. The final concentrations of fibrillogenic peptides were 20 μM for $A\beta_{1-40}$ and $A\beta_{1-42}$ and 44 μM for α-synuclein. Plates were incubated at 37 °C with agitation on a microtiter plate shaker (Glas-Col, Terre Haute, IN), with the speed set to 30 for the time periods indicated. Controls for the fibrillation reactions included carbonic anhydrase (molecular mass of ~29 kDa; C5024, Sigma), a protein chosen because of its comparable weight to 7B2. The development of fibrillation was monitored by measuring the fluorescence of ThT using the SpectraMax M2 fluorometer at 485 nm emission (444 nm excitation).

Dot Blot Analysis—Fibrillated $A\beta_{1-42}$ samples were centrifuged, transferred to a nitrocellulose membrane, and subjected to anti-Aβ Western blot analysis. $A\beta_{1-42}$ fibrillation assays were performed as described above. At 48 h, samples of $A\beta_{1-42}$ control reactions and of reactions incubated with 27- or 21-kDa 7B2 were removed. One-third of each reaction was used as a reference for the total reaction, whereas the remaining material

Downloaded from http://www.jbc.org/ at YONSEI UNIVERSITY on May 20, 2014

was centrifuged for 30 min at 20,000 × g (4 °C) to separate soluble material containing mono- and oligomeric $A\beta_{1-42}$ and pelletable material containing heavy fibrils. An appropriate volume of PBS was added to the total, supernatant, and pellet samples to make the volume up to 100 μl. Ten μl of these reactions were transferred to a 0.2-μm nitrocellulose membrane (Bio-Rad) and air-dried, and the membrane was then blocked with 0.5% BSA and 0.2% goat serum in Tris-buffered saline containing 0.3% Triton X-100. The blot was incubated with monoclonal anti-Aβ antiserum (6E10; 1:1000; Covance) in blocking buffer overnight at 4 °C. On the following day, the blots were washed three times with TBS containing 0.05% Tween 20, followed by incubation at room temperature for 1.5 h using horseradish peroxidase conjugate as the secondary antibody. Blots were incubated with SuperSignal West Pico chemiluminescent substrate (Pierce) for 1 min, and chemiluminescent bands were visualized using HyBlot CL autoradiography film (Denville Scientific Inc.). Dot intensities were analyzed using NIH ImageJ densitometric analysis software and displayed as mean intensity ($n = 3$/group), and the ratios between the supernatant and pellet samples were calculated.

Transmission Electron Microscopy—Specimens (incubated for 72 h) were adsorbed onto 400-mesh Formvar-coated copper grids and negatively stained with 2% phosphotungstic acid (pH 7). After wicking off excess solution, grids were air-dried and examined in a Tecnai T12 transmission electron microscope (FEI) operated at 80 kV. Digital images were acquired using an AMT bottom-mount CCD camera and AMT600 software.

Luciferase Refolding Assay—A possible ATP-dependent, chaperone-like protein-refolding function of 7B2 was tested by incubating unfolded firefly luciferase with recombinant 21- and 27-kDa 7B2, followed by measurement of regained luciferase activity. A 10 μM solution of *Photinus pyralis* luciferase (Roche Applied Science) was resuspended in 0.5 M Tris acetate buffer (pH 7.5), followed by denaturation in 6 M guanidine hydrochloride and 5 mM DTT for 30 min at room temperature. The guanidine hydrochloride solution was dialyzed against PBS overnight at 4 °C. Refolding reactions were performed by diluting denatured luciferase 1:100 in refolding buffer (25 mM HEPES (pH 7.4), 5 mM $MgCl_2$, 50 mM KCl, 5 mM DTT, and 3 mM ATP) in the presence or absence of recombinant 21- or 27-kDa 7B2 (4 μM) using BSA as a negative control and human recombinant HSP70 (Enzo Life Sciences, Farmingdale, NY) as a positive control. The incubation with 7B2 was performed for 3 h at room temperature, followed by 1:10 dilution of reactions into luciferase assay buffer (Promega). Luciferase activity was determined by measurement of luciferin bioluminescence using a FlexStation 3 microplate reader (Molecular Devices). Protein refolding was defined as recovery of luciferase activity expressed as a percent of the activity of native luciferase measured at the same concentration.

Statistical Analysis—Data were analyzed with one- or two-way analysis of variance, followed by the Student-Newman-Keuls multiple comparison test, as appropriate, using a statistical software package (SigmaStat, Systat Software, Inc., San Jose, CA). Data not meeting a normal distribution were analyzed using one-way analysis of variance, followed by the Newman-Keuls multiple comparison test. $p < 0.05$ was considered statistically significant.

RESULTS

7B2 Co-localizes with $A\beta_{1-42}$ Amyloid Plaque Pathology in APP/PSEN1 Mice—To assess a possibly physiologically relevant relationship between 7B2 and proteins involved in amyloid plaque pathology, we performed an immunohistochemical co-localization study using brains from 12-month-old APP mutant mice. Immunoreactive 7B2 was observed in association with $A\beta_{1-42}$ immunoreactivity throughout the brain. Within the hippocampus, 7B2 immunoreactivity strongly overlapped with staining for $A\beta_{1-42}$ (Fig. 1*A*). Furthermore, within the hippocampus, 7B2 immunoreactivity strongly co-localized with staining for $A\beta_{1-42}$ dense core plaque pathology, as demonstrated by its apparent overlap with methoxy-X04-positive $A\beta_{1-42}$ aggregates (Fig. 1*B*).

7B2 Co-localizes with $A\beta_{1-42}$ Deposits in Human AD Hippocampus and with α-Synuclein-rich Lewy Bodies within the Substantia Nigra of a PD Patient—7B2 immunoreactivity was detected throughout the extent of the human brain, including somata and dendritic and axonal branches in neurons of the cortex and mesencephalon (data not shown). Within the hippocampus of a human AD brain, 7B2 strongly co-localized with extracellular $A\beta_{1-42}$ deposits (Fig. 2*A*). 7B2 strongly co-localized with α-synuclein-positive cytoplasmic inclusions (Lewy bodies) in neurons within the substantia nigra of a PD brain (Fig. 2*B*). Although >80% of the observed 7B2 co-localized with α-synuclein immunoreactivity, scattered α-synuclein immunoreactivity could be observed that was not 7B2-immunoreactive (*arrowhead* with *asterisk*). In a similar hippocampus sample from a healthy human control, 7B2 staining was found near cell nuclei, indicating intracellular localization, whereas no significant staining for $A\beta_{1-42}$ could be observed, demonstrating no plaque pathology (Fig. 2*C*).

7B2 Counteracts the Neurocytotoxic Effect of $A\beta_{1-42}$ and Increases Cell Viability—To investigate whether 7B2 is neuroprotective, we performed cell toxicity assays using Neuro-2A cells. A 48-h treatment of Neuro-2A cells with $A\beta_{1-42}$ produced an ~50% decrease in the number of living cells as revealed by quantification of viable cells using both WST-1 assays (Fig. 3*A*, *left panel*) and calcein AM staining (*right panels*). Inclusion of 27- and 21-kDa 7B2 in the medium of Neuro-2A cells during Aβ treatment significantly diminished Aβ-induced cell death. This effect was more pronounced when the 27-kDa form of 7B2 was added and was dose-dependent. $A\beta_{1-42}$-induced cell death was completely prevented when 27-kDa 7B2 was added to the medium together with $A\beta_{1-42}$. Neither of the negative controls, carbonic anhydrase (a similarly sized cytosolic protein) or α-lactalbumin (an irrelevant secreted protein), reduced Aβ neurotoxicity; however, α-crystallin, a known chaperone for Aβ (31, 32), was also able to block toxicity (data not shown).

To determine whether endogenously expressed 7B2 can also prevent Aβ neurotoxicity, we overexpressed 7B2 via adenoviral infection of Neuro-2A cells. A neuroprotective effect was observed when 7B2 was overexpressed by 3-fold (Fig. 3*B*), resulting in a significant increase in living cells, which reached

Downloaded from http://www.jbc.org/ at YONSEI UNIVERSITY on May 20, 2014

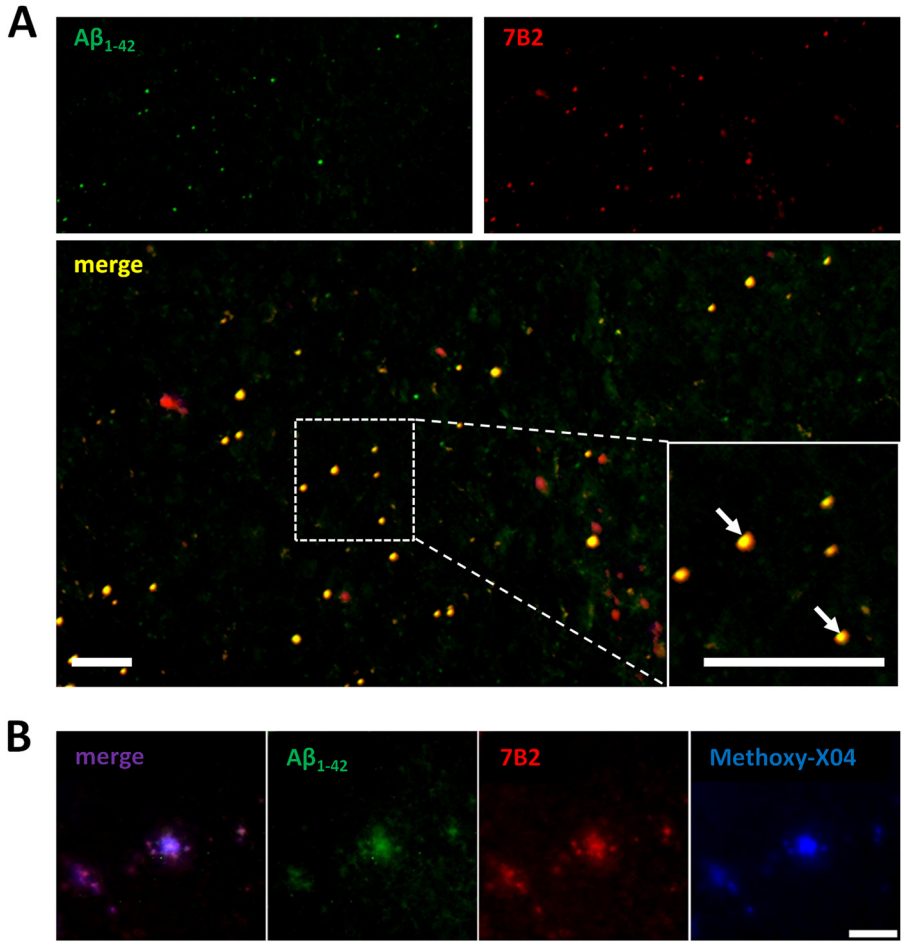

FIGURE 1. **7B2 co-localizes with amyloid plaque pathology.** *A*, the hippocampus of a 12-month-old mutant APP/PSEN1 mouse strongly stained for $A\beta_{1-42}$ immunoreactivity. A composite image shows significant overlap between $A\beta_{1-42}$ (*green*)and 7B2 (*red*) immunoreactivity, resulting in a *yellow* color in the merged image (*arrows*). *Scale bars* = 100 μm. *B*, staining showing significant co-localization (overlap resulting in *purple* hue) of 7B2 (*red*) with $A\beta_{1-42}$ (*green*) and genuine extracellular plaques (*blue*) in the cortices of APP/PSEN1 mice. Plaques were visualized by staining with the *in vivo* amyloid-imaging fluorophore methoxy-X04.

~85% of untreated controls; these results indicate that endogenously expressed 7B2 can rescue cells from $A\beta_{1-42}$-induced neurotoxicity (Fig. 3*C*). In a parallel experiment, we decreased intracellular 7B2 levels using 7B2-specific siRNA. The siRNA-induced decrease in 7B2 was accompanied by a similar decrease in the number of viable Neuro-2A cells; control oligonucleotides showed no such deleterious effect. We observed some co-localization of exogenously added recombinant His-tagged 7B2 with Alexa Fluor-labeled $A\beta_{1-42}$ within Neuro-2A cells (Fig. 3*D*), indicating cellular uptake of both proteins into the cytosol of Neuro-2A cells.

7B2 Inhibits the Fibrillation of $A\beta_{1-42}$, $A\beta_{1-40}$, and α-Synuclein in Vitro—To elucidate the molecular mode of action by which 7B2 inhibits the formation of cytotoxic Aβ species and to obtain structure-function information, we performed *in vitro* fibrillation assays. The addition of full-length 27-kDa 7B2 (structure shown in Fig. 4*A*) inhibited the fibrillation of $A\beta_{1-42}$ at 7B2:$A\beta_{1-42}$ molar ratios of 1:10. Structure-function analysis using truncated forms of 7B2 revealed that this anti-aggregation effect was greatest when the protein was full-length (Fig. 4*B*) and moreover was dose-dependent (Fig. 4*C*). In agreement with these findings, the majority of $A\beta_{1-42}$ became insoluble during the course of the fibrillation assay, as shown by dot blot analysis of centrifugally separated $A\beta_{1-42}$ fibrillation reaction samples, which indicated greater formation of aggregates following 48 h of incubation (Fig. 4*D*). However, the ratio of soluble/lighter $A\beta_{1-42}$ to insoluble/heavier $A\beta_{1-42}$ oligomers (supernatant:pellet) shifted to favor soluble $A\beta_{1-42}$ species when reactions were co-incubated with either 21- or 27-kDa 7B2, suggesting inhibition of the generation of larger fibrils by these proteins. Blockade of fibril formation was independently substantiated by quantification of transmission electron microscope images of $A\beta_{1-42}$ fibrils and oligomers (Fig. 4*E*) incubated at 37 °C for 48 h, which demonstrated a substantial decrease in fibril length when 27-kDa 7B2 was added to the reaction. Although fibrils in the untreated $A\beta_{1-42}$ samples reached an average length of 575 ± 302 nm (mean ± S.D., n = 10) following incubation, fibril length decreased by ~80% when 7B2 was included in the reaction (to 124 ± 233 nm). In these samples, we also observed an increase in the number of smaller spherical $A\beta_{1-42}$ aggregates with an average diameter of 10 ± 4 nm.

The addition of 7B2 to preincubated $A\beta_{1-42}$ samples (at the time point indicated by an arrow) did not result in the disintegration of preformed $A\beta_{1-42}$ fibrils (Fig. 5*A*), indicating that 7B2 does not function as a disaggregase. However, consistent

Downloaded from http://www.jbc.org/ at YONSEI UNIVERSITY on May 20, 2014

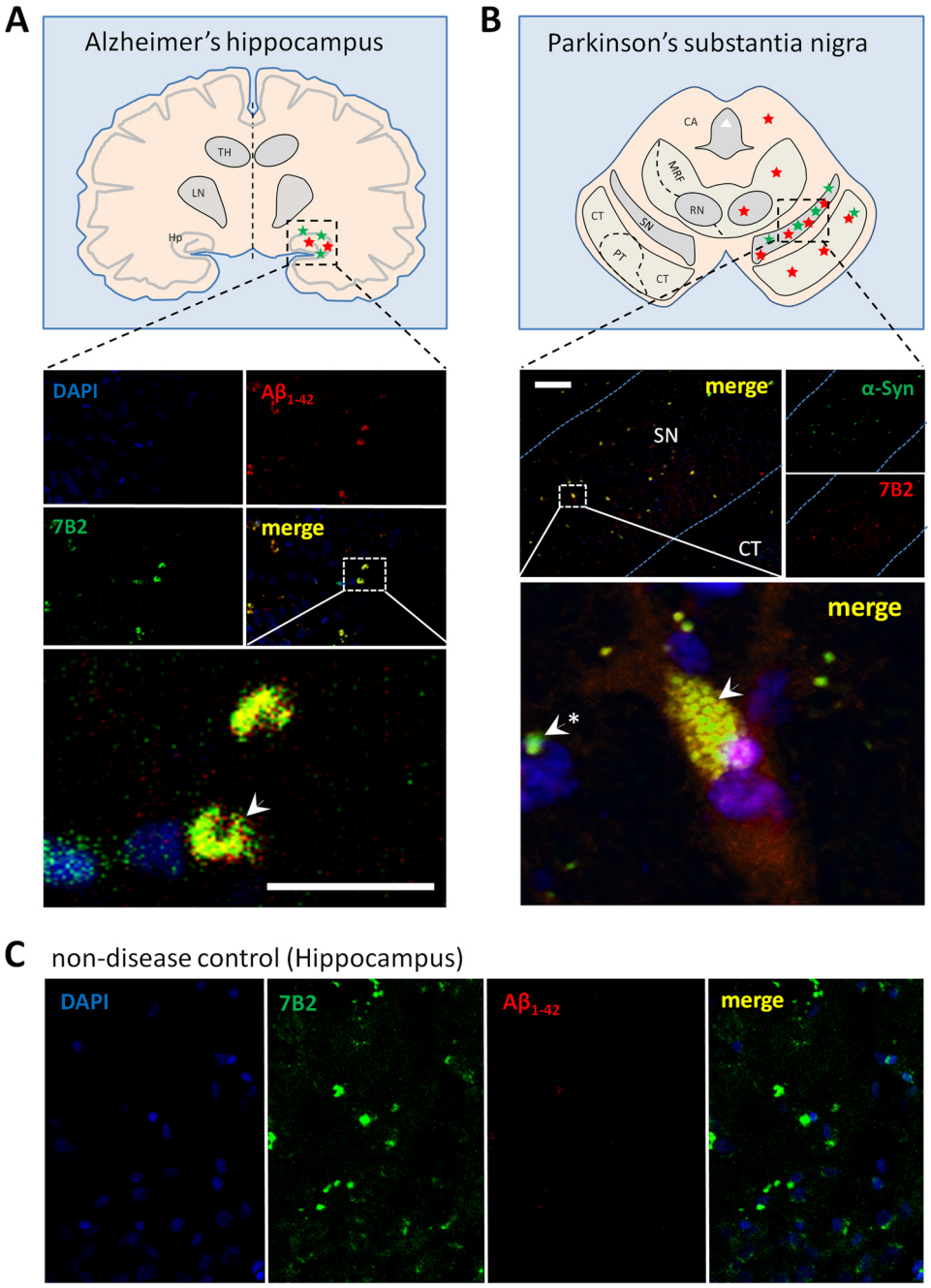

FIGURE 2. **Co-localization of 7B2 with extra- and intracellular protein aggregates in AD hippocampus and PD Lewy bodies.** *A*, AD brain: schematic representation of 7B2 immunoreactivity (*red stars*) and Aβ-positive plaques (*green stars*) as detected throughout the extent of the human brain sample at the level of the hippocampus. *Upper panels*, low magnification images provide an overview of the areas of Aβ-immunoreactive deposits (*red*) and 7B2 expression (*green*) within in the hippocampus. *Lower panel*, high magnification image of representative amyloid plaques within the hippocampus confirms a high degree of co-localization (*arrowhead*) of 7B2 immunoreactivity with Aβ immunoreactivity. *B*, PD brain: 7B2 immunoreactivity (*red stars*) was found throughout the mesencephalon, whereas Lewy bodies were confined to the substantia nigra (*green stars*). *Upper panels*, low magnification images provide an overview of the areas of α-synuclein-immunoreactive deposits in Lewy bodies (*green*) and 7B2 expression (*red*) within the substantia nigra. *Lower panel*, high magnification image of representative Lewy bodies within the substantia nigra confirms a high degree of co-localization (*arrowhead*) of 7B2 immunoreactivity with α-synuclein immunoreactivity. The majority of 7B2 immunoreactivity was confined to areas near the nucleus, suggesting intracellular localization. *C*, 7B2 immunoreactivity was detected in a human control brain sample. Shown are representative images of the hippocampus in a non-diseased control brain. Although only limited Aβ immunoreactivity (*red*) and no plaque burden were detected, we observed significant 7B2 immunoreactivity (*green*) that was confined to areas near cell nuclei, suggesting intracellular localization. *CA*, cerebral aqueduct; *CT*, corticopontine tract; *Hp*, hippocampus; *LN*, lentiform nucleus; *MRF*, mesencephalic reticular formation; *PT*, pyramidal tract; *RN*, red nucleus; *SN*, substantia nigra; *TH*; thalamus. *Scale bars* = 10 μm.

with its effects on $A\beta_{1-42}$ fibrillation, 7B2 also inhibited the formation of $A\beta_{1-40}$ (Fig. 5*B*) and α-synuclein fibrils (Fig. 5*C*). A dose-dependent relationship was observed for blockade of α-synuclein fibrillation by 27-kDa 7B2 (Fig. 5*D*).

We next aimed to determine whether 7B2 exhibits ATP-dependent chaperone-like refolding properties similar to those of larger chaperones such as members of the HSP70 and HSP90 families. Although denatured luciferase was efficiently refolded

Downloaded from http://www.jbc.org/ at YONSEI UNIVERSITY on May 20, 2014

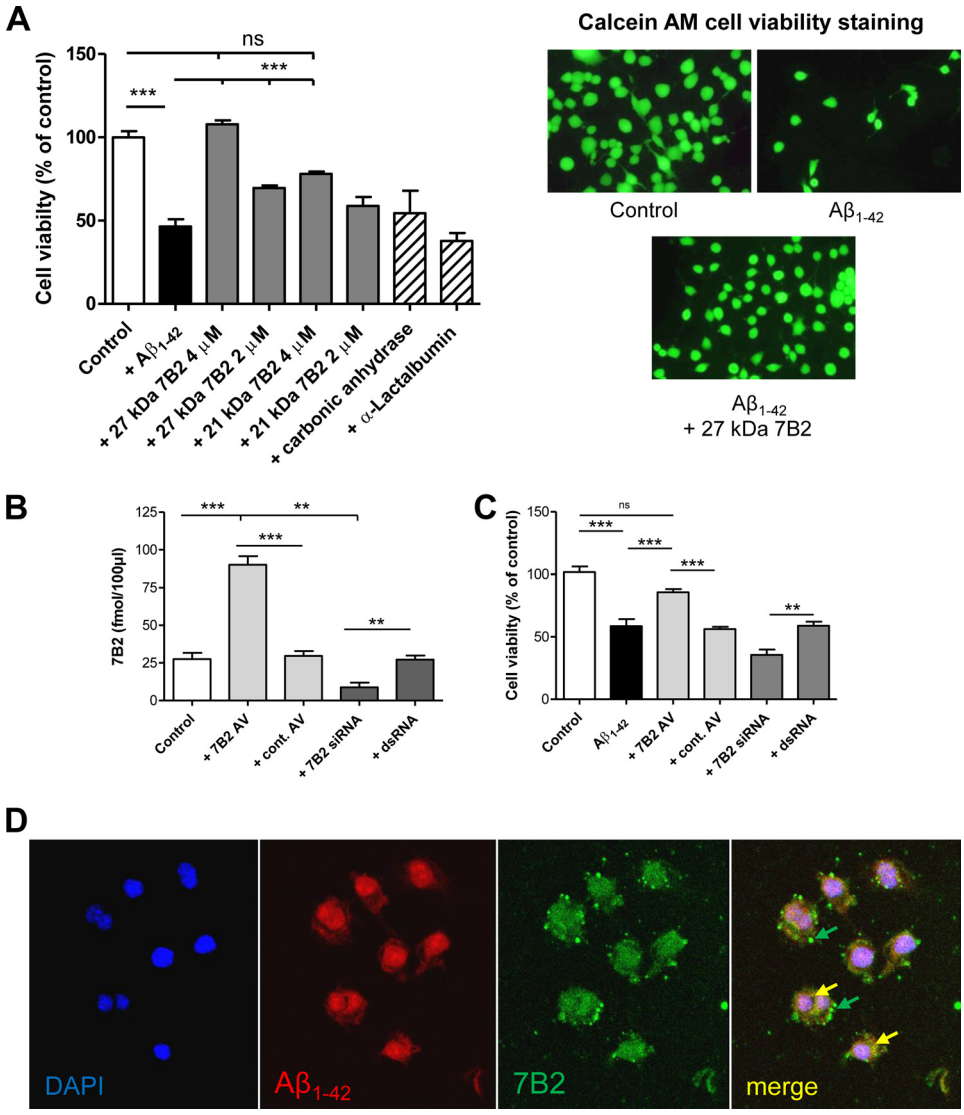

FIGURE 3. **7B2 decreases Aβ-induced cell death in Neuro-2A cells.** *A*, Neuro-2A cells were treated with 10 μM $A\beta_{1-42}$ for 48 h to induce cell death in the presence or absence of 7B2. *Left panel*, quantification of Aβ-induced cell death by the WST-1 cell viability assay. *Right panels*, representative photomicrographs showing viable calcein AM-stained Neuro-2A cells following treatment with $A\beta_{1-42}$ with or without 7B2. *ns*, not significant. *B*, quantification of endogenous 7B2 levels in Neuro-2A cells by radioimmunoassay following either adenoviral (*AV*) overexpression or RNAi-mediated knockdown. *cont.*, control. *C*, $A\beta_{1-42}$-induced cell death following manipulation of intracellular 7B2 levels was monitored using the WST-1 cell viability assay. *D*, exogenously added recombinant His-tagged 7B2 (*green arrows*) was internalized and co-localized with Alexa Fluor-labeled $A\beta_{1-42}$ (*red*) in Neuro-2A cells, indicating co-uptake into the cytosol of Neuro-2A cells (*yellow arrows*). Anti-His tag antiserum was used for the experiment in *D*.

by HSP70, restoring about half of its enzymatic function, 7B2 displayed no significant refolding activity (Fig. 6).

The small molecular mass of 7B2 potentially qualifies this protein to be classified as a small heat shock protein; these chaperone proteins possess masses between 15 and 40 kDa and share the conserved sequence known as the α-crystallin domain (33). However, multisequence alignment using 3D/T-Coffee Web server tools revealed no significant sequence identity to either α-crystallin itself or the comparably sized heat shock protein sHSP27 (data not shown).

DISCUSSION

Neurodegenerative diseases such as AD and PD have been established as "protein-folding disorders," the etiology of which involves the aggregation of non-native protein conformations, resulting in extracellular and intracellular protein aggregates (34). The abundance of these protein aggregates in neurodegenerative disease is, however, difficult to explain and appears to represent an essential failure of neuronal chaperone systems to sustain native protein conformation. The particular toxicity of protein aggregates in the nervous system implies that neurons may require special mechanisms to maintain continuous chaperone control of protein aggregation during secretory pathway transit, granule residence, and even following secretion and reuptake, yet few specifically neuronal secretory chaperone mechanisms have been described.

Although 7B2 has long been recognized as an excellent neuroendocrine marker involved in PC2-mediated peptide synthesis (13, 14), its widespread neuronal distribution within the brain, and also in areas lacking prohormone convertases (15), strongly suggests non-convertase-related functions. Our immunohistochemical data show clear co-localization of 7B2

Downloaded from http://www.jbc.org/ at YONSEI UNIVERSITY on May 20, 2014

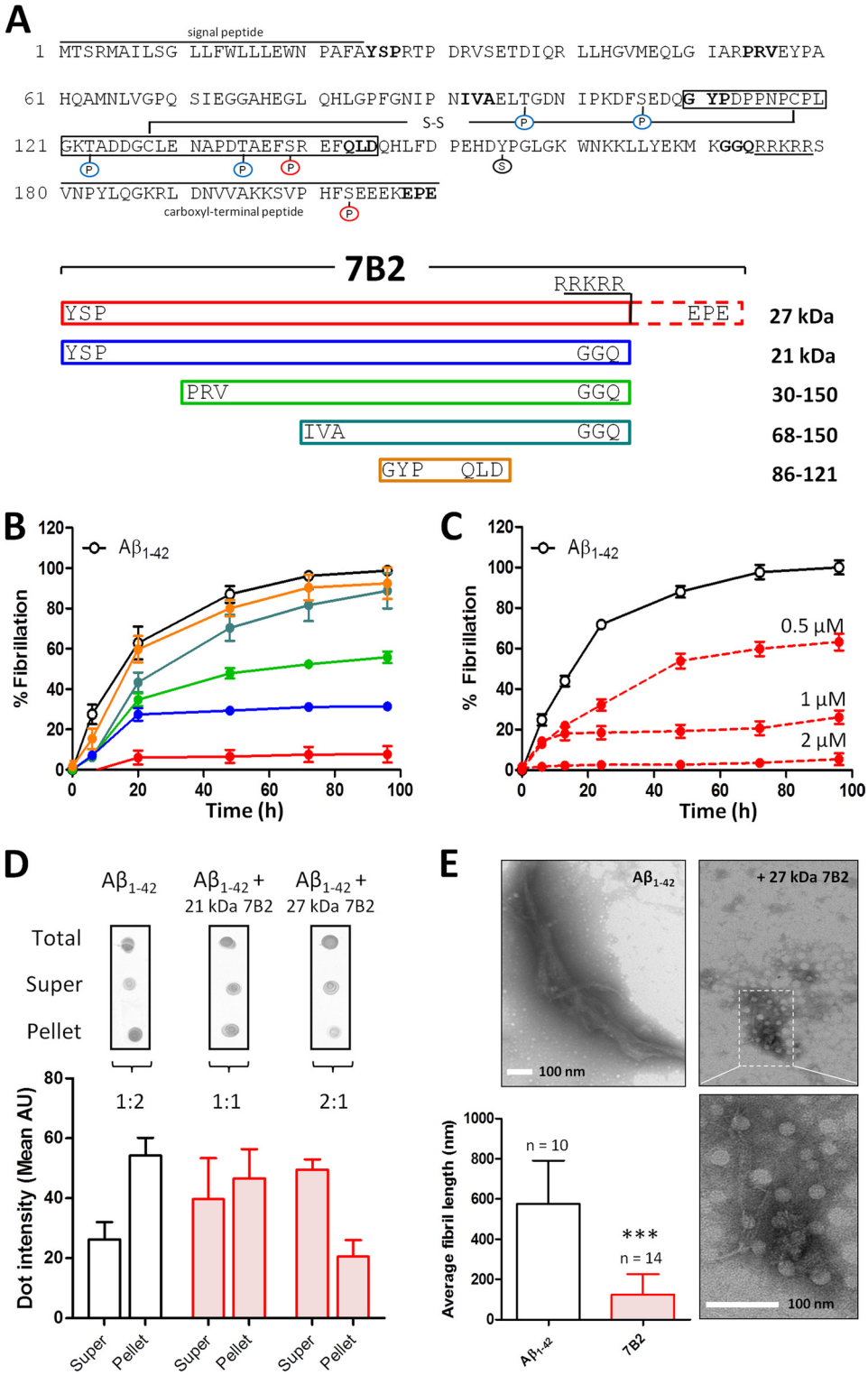

FIGURE 4. **Structure-function analysis of 7B2 proteins in suppressing Aβ fibrillation.** *A*, *upper*, amino acid sequence of rat 7B2 including the N-terminal signal peptide and the C-terminal inhibitory peptide domain. Putative post-translational modification sites are marked (*red P*, known phosphorylation site; *blue P*, hypothetical phosphorylation site; *black S*, sulfation; *S-S*, disulfide bond); the C-terminal cleavage site is *underlined*; and the minimal amino acid sequence required for PC2 activation is *boxed*. The first and last three amino acids of the 7B2 fragments used in this study are indicated in *boldface*. *Lower*, domain structure of 7B2 and schematic representation of the N-terminal deletions and peptides used in this study. *B*, $A\beta_{1-42}$ (20 μM) was incubated with either full-length 7B2 (27 kDa; *red*) or truncated proteins and peptides (2 μM). Protein fibrillation was monitored using a ThT fibrillation assay. *C*, the inhibition of $A\beta_{1-42}$ aggregation in the presence of 27-kDa 7B2 was dose-dependent and was most effective at a 7B2:$A\beta_{1-42}$ molar ratio of 1:10. *D*, quantification of supernatant (soluble $A\beta_{1-42}$) *versus* pellet (insoluble $A\beta_{1-42}$) dot intensities revealed a ratio shift (supernatant:pellet) toward the soluble $A\beta_{1-42}$ species following the addition of 7B2. *AU*, absorbance units. *E*, quantification of $A\beta_{1-42}$ fibril formation observed after 72 h of incubation in reactions with or without 7B2 by transmission electron microscopy. ***, $p < 0.001$.

Downloaded from http://www.jbc.org/ at YONSEI UNIVERSITY on May 20, 2014

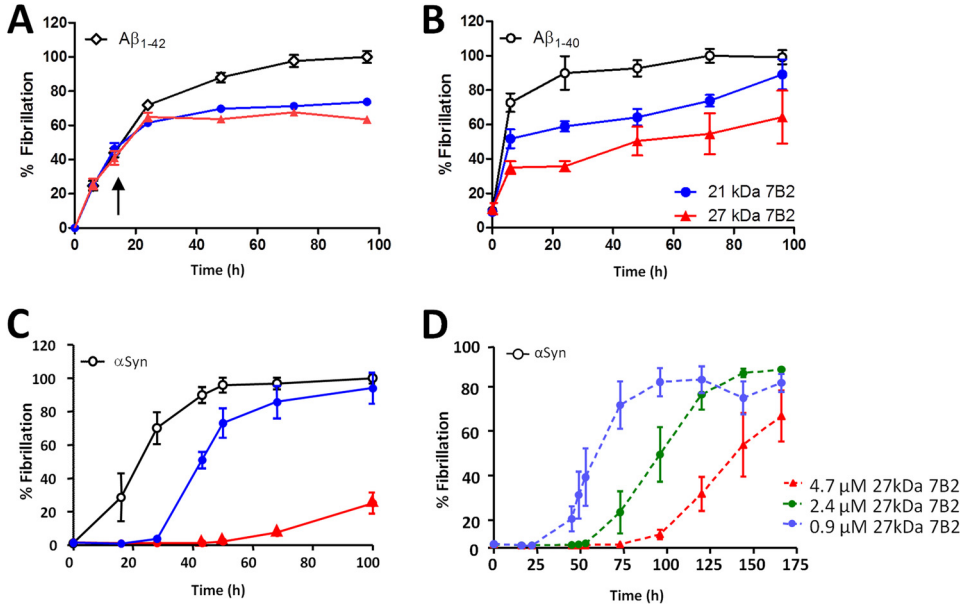

FIGURE 5. **7B2 does not disintegrate preformed mature $A\beta_{1-42}$ fibrils but suppresses $A\beta_{1-40}$ and α-synuclein fibrillation.** *A*, $A\beta_{1-42}$ (20 μM) was incubated at 37 °C, followed by the addition of 2 μM 27- or 21-kDa 7B2 at the time point indicated by the *arrow*. Protein aggregation was monitored with the ThT fibrillation assay. Further $A\beta_{1-42}$ aggregation was inhibited once 7B2 was added; however, preformed mature fibrils were not affected (n = 3/group). $A\beta_{1-40}$ (20 μM) (*B*) and α-synuclein (*αSyn*; 44 μM) (*C*) were incubated with full-length 7B2 (27 kDa; *red*) or 21-kDa 7B2 (*blue*), respectively, and fibrillation was monitored by the ThT assay. *D*, dose dependence relationship for inhibition of α-synuclein fibrillation by 27-kDa 7B2.

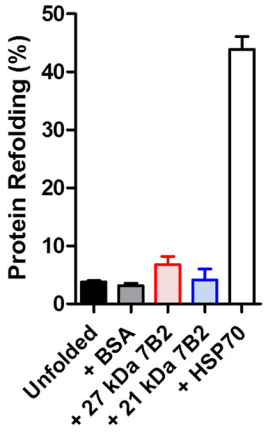

FIGURE 6. **7B2 does not possess chaperone-like refolding activity.** Unfolded and inactive firefly luciferase (40 μM) was incubated with either 21- or 27-kDa 7B2 (4 μM), followed by measurement of regained (refolded) luciferase enzyme activity, determined by luciferin bioluminescence assay.

with aggregated proteins in neurodegenerative disease, indicating a potential functional relationship. A similar accumulation of chaperones within amyloid-like plaques in the brains of AD and PD patients has been reported for α-crystallin, HSP47, and clusterin (8, 35, 36). Interestingly, the distribution of immunoreactive 7B2 in diseased brain indicates that this protein may possess a higher affinity for non-aggregated $A\beta_{1-40}$, $A\beta_{1-42}$, and $A\beta_{1-40}$ and a lesser affinity for fully mature dense core plaques. This suggests an anti-aggregation effect of 7B2 that is temporally organized, occurring prior to compaction of Aβ deposits, as would be expected from a chaperone-mediated defense response to Aβ plaque maturation. A general association of 7B2 with neurodegenerative protein aggregation is further substantiated by the pronounced intracellular co-localization of 7B2 with α-synuclein-rich Lewy bodies within the substantia nigra of a PD patient.

7B2 is found together with intracellular and extracellular protein aggregates, implying that it could act at both locations. We speculate that 7B2 may block inappropriate protein-protein interactions initially during intracellular protein trafficking through the secretory pathway, extracellularly following secretion of 7B2 and Aβ, and possibly even following reuptake. Interestingly, cellular reuptake of Aβ into endosomes and lysosomes has been reported to facilitate its aggregation (37). Here, we have shown that Neuro-2A cells are capable of taking up added Aβ simultaneously with added exogenous 7B2, raising the idea that these compartments serve as sites for 7B2 interaction with Aβ under physiological conditions. The cytoplasmic protein α-synuclein has been reported to be secreted and to be localized intravesicularly in a similar fashion (38); an analogous mechanism could be operative for α-synuclein/7B2. However, whether extracellular association of these proteins occurs prior to uptake or whether both species are nonspecifically endocytosed together is not yet clear.

We have further demonstrated here that added 7B2 can block the cytotoxic effects of Aβ peptides. Neuro-2A cells exposed to toxic Aβ oligomers died rapidly; inclusion of either 7B2 or α-crystallin, but not the control proteins carbonic anhydrase and α-lactalbumin, blocked the cytotoxic effects of these oligomers. It is unlikely that fibril formation is involved in Aβ neurotoxicity because the concentration of Aβ used was low (10 μM) and because Aβ oligomers appear to be much more toxic than fibrils (39). Thus, 7B2 may function to block protein-protein association at the oligomer level; this idea is in line with the known ability of 7B2 to block both the oligomerization and the aggregation of the convertase proPC2 (18).

Of great physiological importance is our observation that modulation of intracellular 7B2 expression directly correlates with the cytotoxicity of exogenously administered $A\beta_{1-42}$. In a

Downloaded from http://www.jbc.org/ at YONSEI UNIVERSITY on May 20, 2014

similar approach, Magrané *et al.* (40) have shown that viral overexpression of HSP70 successfully rescues neurons from the toxic effects of intracellular Aβ accumulation. Moreover, another study demonstrated that drug-induced chaperone overexpression of HSP70 and HSP90 maintains tau protein in a soluble and functional conformation, preventing it from aggregating (10). In line with these studies, our data indicate that a certain level of endogenous 7B2 may be sufficient to prevent the formation of harmful Aβ_{1-42} species and support the idea that loss of neuronal 7B2 might facilitate Aβ_{1-42}-induced neurotoxicity. The location of 7B2 action in blocking Aβ_{1-42}-induced neurotoxicity requires further investigation; it is possible that 7B2 acts both extracellularly to block oligomer formation and intracellularly following reuptake.

In addition to these *in vivo* and cellular data linking 7B2 with the toxic effects of Aβ, we have directly demonstrated that 7B2 suppresses the fibrillation of aggregation-prone proteins *in vitro*. The ability of 7B2 to act at low stoichiometric ratios with respect to client proteins is remarkable and further supports the idea of 7B2 involvement in Aβ-related plaque formation.

Most protein chaperones described to date function intracellularly. Only four secreted chaperones that act extracellularly have been identified thus far: (i) the ubiquitously expressed glycoprotein clusterin/ApoJ, which in the brain appears to be of glial origin (11); (ii) the heat shock-related lens protein α-crystallin (41); (iii) the presumed Aβ chaperone prostaglandin D synthase/β-trace (42); and the receptor-associated protein RAP (43). Of these, the chaperone with by far the greatest genetic association with AD is clusterin (reviewed in Refs. 11 and 12). A key feature that distinguishes 7B2 from clusterin is that clusterin is expressed in nearly all mammalian tissues, whereas 7B2 expression is limited to cells containing a regulated secretory pathway: the central and peripheral nervous systems and endocrine/neuroendocrine systems. Interestingly, a recent study investigating the interaction of clusterin and Aβ using biophysical approaches reported that clusterin binds to and stabilizes Aβ oligomers of all sizes, thereby influencing the equilibrium of Aβ oligomers, aggregates, and fibrils (44). It is possible that 7B2 acts via similar molecular mechanisms to decrease Aβ protein oligomerization, fibrillation, and cytotoxicity. The appearance of the disc-shaped structures observed by electron microscopy in this study seems to represent an increase in spherical Aβ_{1-42} oligomers, potentially indicating that 7B2 promotes the formation of nontoxic stable off-pathway Aβ species, similar to what has been reported following treatment with inositol (45).

Biophysical characterization of recombinant 7B2 has shown that it is an intrinsically disordered protein capable of oligomerization (46). These properties are similar to those of certain small anti-aggregant cytosolic heat shock proteins (reviewed in Refs. 47 and 48), and we speculate that 7B2 may block the formation of protein aggregates using similar mechanisms. Although weak homology to chaperonin-related sequences has been reported (17), 7B2 exhibits no significant sequence homology to clusterin, crystallins, or small heat shock proteins. Thus, 7B2 appears to have novel anti-aggregation domains. The role of the known post-translational modifications of this protein, sulfation (49) and phosphorylation (50, 51) (see Fig. 4*A*), in anti-aggregation remains to be established.

In summary, our data provide new insight into the function of neuronal 7B2 and establish this protein as a novel anti-aggregation chaperone strongly associated with neurodegenerative disease. Interestingly, recent proteomics studies also point to an association of 7B2 with various neurodegeneration-related protein-misfolding diseases, including AD, PD, and amyotrophic lateral sclerosis (20–23). These observations are supported by data showing that 7B2 is significantly up-regulated in brain tissues of AD patients (52) and by a fifth proteomics study in which 7B2 was found to be elevated in the cerebrospinal fluid of amyotrophic lateral sclerosis patients (53), indicating possible up-regulation of 7B2 as a response to increased protein aggregation and misfolding. Taken together with the work presented here, these studies provide support for the idea that 7B2 plays a role in the etiology of aggregate formation in neurodegenerative disease.

Acknowledgments—We acknowledge the technical support of the Core Imaging Facility, the UMB Biopolymer Core Lab for Peptide Synthesis, and the NICHD Brain and Tissue Bank for Developmental Disorders of the University of Maryland, Baltimore.

REFERENCES

1. Ross, C. A., and Poirier, M. A. (2004) Protein aggregation and neurodegenerative disease. *Nat. Med.* **10,** S10–S17
2. Glenner, G. G., and Wong, C. W. (1984) Alzheimer's disease: initial report of the purification and characterization of a novel cerebrovascular amyloid protein. *Biochem. Biophys. Res. Commun.* **120,** 885–890
3. Kosik, K. S., Joachim, C. L., and Selkoe, D. J. (1986) Microtubule-associated protein tau (tau) is a major antigenic component of paired helical filaments in Alzheimer disease. *Proc. Natl. Acad. Sci. U.S.A.* **83,** 4044–4048
4. Spillantini, M. G., Schmidt, M. L., Lee, V. M., Trojanowski, J. Q., Jakes, R., and Goedert, M. (1997) α-Synuclein in Lewy bodies. *Nature* **388,** 839–840
5. Pike, C. J., Walencewicz, A. J., Glabe, C. G., and Cotman, C. W. (1991) *In vitro* aging of β-amyloid protein causes peptide aggregation and neurotoxicity. *Brain Res.* **563,** 311–314
6. Muchowski, P. J., and Wacker, J. L. (2005) Modulation of neurodegeneration by molecular chaperones. *Nat. Rev. Neurosci.* **6,** 11–22
7. Nemes, Z., Devreese, B., Steinert, P. M., Van Beeumen, J., and Fésüs, L. (2004) Cross-linking of ubiquitin, HSP27, parkin, and α-synuclein by γ-glutamyl–ϵ-lysine bonds in Alzheimer's neurofibrillary tangles. *FASEB J.* **18,** 1135–1137
8. Renkawek, K., Bosman, G. J., and de Jong, W. W. (1994) Expression of small heat-shock protein hsp 27 in reactive gliosis in Alzheimer disease and other types of dementia. *Acta Neuropathol.* **87,** 511–519
9. McLean, P. J., Kawamata, H., Shariff, S., Hewett, J., Sharma, N., Ueda, K., Breakefield, X. O., and Hyman, B. T. (2002) TorsinA and heat shock proteins act as molecular chaperones: suppression of α-synuclein aggregation. *J. Neurochem.* **83,** 846–854
10. Dou, F., Netzer, W. J., Tanemura, K., Li, F., Hartl, F. U., Takashima, A., Gouras, G. K., Greengard, P., and Xu, H. (2003) Chaperones increase association of tau protein with microtubules. *Proc. Natl. Acad. Sci. U.S.A.* **100,** 721–726
11. Jones, S. E., and Jomary, C. (2002) Clusterin. *Int. J. Biochem. Cell Biol.* **34,** 427–431
12. Wu, Z. C., Yu, J. T., Li, Y., and Tan, L. (2012) Clusterin in Alzheimer's disease. *Adv. Clin. Chem.* **56,** 155–173
13. Mbikay, M., Seidah, N. G., and Chrétien, M. (2001) Neuroendocrine secretory protein 7B2: structure, expression and functions. *Biochem. J.* **357,** 329–342
14. Muller, L., and Lindberg, I. (1999) The cell biology of the prohormone convertases PC1 and PC2. *Prog. Nucleic Acid Res. Mol. Biol.* **63,** 69–108
15. Seidel, B., Dong, W., Savaria, D., Zheng, M., Pintar, J. E., and Day, R. (1998)

Downloaded from http://www.jbc.org/ at YONSEI UNIVERSITY on May 20, 2014

Neuroendocrine protein 7B2 is essential for proteolytic conversion and activation of proprotein convertase 2 *in vivo*. *DNA Cell Biol.* **17,** 1017–1029
16. Iguchi, H., Chan, J. S. D., Seidah, N. G., and Chrétien, M. (1984) Tissue distribution and molecular forms of a novel pituitary protein in the rat. *Neuroendocrinology* **39,** 453–458
17. Braks, J. A. M., and Martens, G. J. M. (1994) 7B2 is a neuroendocrine chaperone that transiently interacts with prohormone convertase PC2 in the secretory pathway. *Cell* **78,** 263–273
18. Lee, S.-N., and Lindberg, I. (2008) 7B2 prevents unfolding and aggregation of prohormone convertase 2. *Endocrinology* **149,** 4116–4127
19. Chaudhuri, B., Stephan, C., Huijbregts, R. P., and Martens, G. J. (1995) The neuroendocrine protein 7B2 acts as a molecular chaperone in the *in vitro* folding of human insulin-like growth factor-1 secreted from yeast. *Biochem. Biophys. Res. Commun.* **211,** 417–425
20. Jahn, H., Wittke, S., Zürbig, P., Raedler, T. J., Arlt, S., Kellmann, M., Mullen, W., Eichenlaub, M., Mischak, H., and Wiedemann, K. (2011) Peptide fingerprinting of Alzheimer's disease in cerebrospinal fluid: identification and prospective evaluation of new synaptic biomarkers. *PLoS ONE* **6,** e26540
21. Pasinetti, G. M., Ungar, L. H., Lange, D. J., Yemul, S., Deng, H., Yuan, X., Brown, R. H., Cudkowicz, M. E., Newhall, K., Peskind, E., Marcus, S., and Ho, L. (2006) Identification of potential CSF biomarkers in ALS. *Neurology* **66,** 1218–1222
22. Finehout, E. J., Franck, Z., Choe, L. H., Relkin, N., and Lee, K. H. (2007) Cerebrospinal fluid proteomic biomarkers for Alzheimer's disease. *Ann. Neurol.* **61,** 120–129
23. Bayés, A., and Grant, S. G. (2009) Neuroproteomics: understanding the molecular organization and complexity of the brain. *Nat. Rev. Neurosci.* **10,** 635–646
24. Croisier, E., MRes, D. E., Deprez, M., Goldring, K., Dexter, D. T., Pearce, R. K., Graeber, M. B., and Roncaroli, F. (2006) Comparative study of commercially available anti-α-synuclein antibodies. *Neuropathol. Appl. Neurobiol.* **32,** 351–356
25. Stine, W. B., Jungbauer, L., Yu, C., and LaDu, M. J. (2011) Preparing synthetic Aβ in different aggregation states. *Methods Mol. Biol.* **670,** 13–32
26. Helwig, M., Lee, S.-N., Hwang, J. R., Ozawa, A., Medrano, J. F., and Lindberg, I. (2011) Dynamic modulation of PC2-mediated precursor processing by 7B2. Preferential effect on glucagon synthesis. *J. Biol. Chem.* **286,** 42504–42513
27. Muller, L., Zhu, P., Juliano, M. A., Juliano, L., and Lindberg, I. (1999) A 36-residue peptide contains all of the information required for 7B2-mediated activation of prohormone convertase 2. *J. Biol. Chem.* **274,** 21471–21477
28. Zhu, X., Lamango, N. S., and Lindberg, I. (1996) Involvement of a polyproline helix-like structure in the interaction of 7B2 with prohormone convertase 2. *J. Biol. Chem.* **271,** 23582–23587
29. Giasson, B. I., Forman, M. S., Higuchi, M., Golbe, L. I., Graves, C. L., Kotzbauer, P. T., Trojanowski, J. Q., and Lee, V. M. (2003) Initiation and synergistic fibrillization of tau and α-synuclein. *Science* **300,** 636–640
30. Kjaer, A., Knigge, U., Bach, F. W., and Warberg, J. (1995) Stress-induced secretion of pro-opiomelanocortin-derived peptides in rats: relative importance of the anterior and intermediate pituitary lobes. *Neuroendocrinology* **61,** 167–172
31. Raman, B., Ban, T., Sakai, M., Pasta, S. Y., Ramakrishna, T., Naiki, H., Goto, Y., and Rao, Ch. M. (2005) αB-crystallin, a small heat-shock protein, prevents the amyloid fibril growth of an amyloid β-peptide and β_2-microglobulin. *Biochem. J.* **392,** 573–581
32. Tanaka, N., Tanaka, R., Tokuhara, M., Kunugi, S., Lee, Y. F., and Hamada, D. (2008) Amyloid fibril formation and chaperone-like activity of peptides from αA-crystallin. *Biochemistry* **47,** 2961–2967
33. Kim, K. K., Kim, R., and Kim, S. H. (1998) Crystal structure of a small heat-shock protein. *Nature* **394,** 595–599
34. Kopito, R. R., and Ron, D. (2000) Conformational disease. *Nat. Cell Biol.* **2,** E207–E209
35. Bianchi, F. T., Camera, P., Ala, U., Imperiale, D., Migheli, A., Boda, E., Tempia, F., Berto, G., Bosio, Y., Oddo, S., LaFerla, F. M., Taraglio, S., Dotti, C. G., and Di Cunto, F. (2011) The collagen chaperone HSP47 is a new interactor of APP that affects the levels of extracellular β-amyloid peptides. *PLoS ONE* **6,** e22370
36. Sasaki, K., Satomi, Y., Takao, T., and Minamino, N. (2009) Snapshot peptidomics of the regulated secretory pathway. *Mol. Cell. Proteomics* **8,** 1638–1647
37. Hu, X., Crick, S. L., Bu, G., Frieden, C., Pappu, R. V., and Lee, J. M. (2009) Amyloid seeds formed by cellular uptake, concentration, and aggregation of the amyloid-β peptide. *Proc. Natl. Acad. Sci. U.S.A.* **106,** 20324–20329
38. Lee, H. J., Patel, S., and Lee, S. J. (2005) Intravesicular localization and exocytosis of α-synuclein and its aggregates. *J. Neurosci.* **25,** 6016–6024
39. Bieschke, J., Herbst, M., Wiglenda, T., Friedrich, R. P., Boeddrich, A., Schiele, F., Kleckers, D., Lopez del Amo, J. M., Grüning, B. A., Wang, Q., Schmidt, M. R., Lurz, R., Anwyl, R., Schnoegl, S., Fändrich, M., Frank, R. F., Reif, B., Günther, S., Walsh, D. M., and Wanker, E. E. (2012) Small-molecule conversion of toxic oligomers to nontoxic β-sheet-rich amyloid fibrils. *Nat. Chem. Biol.* **8,** 93–101
40. Magrané, J., Smith, R. C., Walsh, K., and Querfurth, H. W. (2004) Heat shock protein 70 participates in the neuroprotective response to intracellularly expressed β-amyloid in neurons. *J. Neurosci.* **24,** 1700–1706
41. Andley, U. P. (2007) Crystallins in the eye: function and pathology. *Prog. Retin. Eye Res.* **26,** 78–98
42. Kanekiyo, T., Ban, T., Aritake, K., Huang, Z. L., Qu, W. M., Okazaki, I., Mohri, I., Murayama, S., Ozono, K., Taniike, M., Goto, Y., and Urade, Y. (2007) Lipocalin-type prostaglandin D synthase/β-trace is a major amyloid β-chaperone in human cerebrospinal fluid. *Proc. Natl. Acad. Sci. U.S.A.* **104,** 6412–6417
43. Kanekiyo, T., and Bu, G. (2009) Receptor-associated protein interacts with amyloid-β peptide and promotes its cellular uptake. *J. Biol. Chem.* **284,** 33352–33359
44. Narayan, P., Orte, A., Clarke, R. W., Bolognesi, B., Hook, S., Ganzinger, K. A., Meehan, S., Wilson, M. R., Dobson, C. M., and Klenerman, D. (2012) The extracellular chaperone clusterin sequesters oligomeric forms of the amyloid-β(1–40) peptide. *Nat. Struct. Mol. Biol.* **19,** 79–83
45. McLaurin, J., Golomb, R., Jurewicz, A., Antel, J. P., and Fraser, P. E. (2000) Inositol stereoisomers stabilize an oligomeric aggregate of Alzheimer amyloid β peptide and inhibit Aβ-induced toxicity. *J. Biol. Chem.* **275,** 18495–18502
46. Dasgupta, I., Sanglas, L., Enghild, J. J., and Lindberg, I. (2012) The neuroendocrine protein 7B2 is intrinsically disordered. *Biochemistry* **51,** 7456–7464
47. Jakob, U., Gaestel, M., Engel, K., and Buchner, J. (1993) Small heat shock proteins are molecular chaperones. *J. Biol. Chem.* **268,** 1517–1520
48. McHaourab, H. S., Godar, J. A., and Stewart, P. L. (2009) Structure and mechanism of protein stability sensors: chaperone activity of small heat shock proteins. *Biochemistry* **48,** 3828–3837
49. Paquet, L., Bergeron, F., Boudreault, A., Seidah, N. G., Chrétien, M., Mbikay, M., and Lazure, C. (1994) The neuroendocrine precursor 7B2 is a sulfated protein proteolytically processed by a ubiquitous furin-like convertase. *J. Biol. Chem.* **269,** 19279–19285
50. Lee, S.-N., Hwang, J. R., and Lindberg, I. (2006) Neuroendocrine protein 7B2 can be inactivated by phosphorylation within the secretory pathway. *J. Biol. Chem.* **281,** 3312–3320
51. Sigafoos, J., Chestnut, W. G., Merrill, B. M., Taylor, L. C. E., Diliberto, E. J., Jr., and Viveros, O. H. (1993) Identification of a 7B2-derived tridecapeptide from bovine adrenal medulla chromaffin vesicles. *Cell. Mol. Neurobiol.* **13,** 271–278
52. Winsky-Sommerer, R., Grouselle, D., Rougeot, C., Laurent, V., David, J. P., Delacourte, A., Dournaud, P., Seidah, N. G., Lindberg, I., Trottier, S., and Epelbaum, J. (2003) The proprotein convertase PC2 is involved in the maturation of prosomatostatin to somatostatin-14 but not in the somatostatin deficit in Alzheimer's disease. *Neuroscience* **122,** 437–447
53. Ranganathan, S., Williams, E., Ganchev, P., Gopalakrishnan, V., Lacomis, D., Urbinelli, L., Newhall, K., Cudkowicz, M. E., Brown, R. H., Jr., and Bowser, R. (2005) Proteomic profiling of cerebrospinal fluid identifies biomarkers for amyotrophic lateral sclerosis. *J. Neurochem.* **95,** 1461–1471
54. Clemente, C. D. (1985) *Gray's Anatomy of the Human Body*, 30th Ed., Lea & Febiger, Philadelphia

Downloaded from http://www.jbc.org/ at YONSEI UNIVERSITY on May 20, 2014